Vol 18 No 9, September 2009
1674-1056/2009/18(09)/4013-06

Chinese Physics B

© 2009 Chin. Phys. Soc.
and IOP Publishing Ltd

Optical properties of hexagonal boron nitride thin films deposited by radio frequency bias magnetron sputtering*

Deng Jin-Xiang(邓金祥)[a)†], Zhang Xiao-Kang(张晓康)[a)b)], Yao Qian(姚 倩)[b)], Wang Xu-Yang(汪旭洋)[a)], Chen Guang-Hua(陈光华)[a)], and He De-Yan(贺德衍)[b)]

[a)] *School of Applied Mathematics and Physics, Beijing University of Technology, Beijing* 100124, *China*
[b)] *School of Physical Science and Technology, Lanzhou University, Lanzhou* 730000, *China*

(Received 15 November 2008; revised manuscript received 13 April 2009)

The optical properties of hexagonal boron nitride (h-BN) thin films were studied in this paper. The films were characterized by Fourier transform infrared spectroscopy, UV–visible transmittance and reflection spectra. h-BN thin films with a wide optical band gap E_g (5.86 eV for the as-deposited film and 5.97 eV for the annealed film) approaching h-BN single crystal were successfully prepared by radio frequency (RF) bias magnetron sputtering and post-deposition annealing at 970 K. The optical absorption behaviour of h-BN films accords with the typical optical absorption characteristics of amorphous materials when fitting is made by the Urbach tail model. The annealed film shows satisfactory structure stability. However, high temperature still has a significant effect on the optical absorption properties, refractive index n, and optical conductivity σ of h-BN thin films. The blue-shift of the optical absorption edge and the increase of E_g probably result from stress relaxation in the film under high temperatures. In addition, it is found that the refractive index clearly exhibits different trends in the visible and ultraviolet regions. Previous calculational results of optical conductivity of h-BN films are confirmed in our experimental results.

Keywords: hexagonal boron nitride films, sputtering, UV–visible, optical properties
PACC: 7865K, 7850G

1. Introduction

There are four common polytypes in the boron nitride system, hexagonal (h-BN), rhombohedral (r-BN), cubic zincblende (c-BN) and wurtzite (w-BN). In the system, hexagonal boron nitride (h-BN) is the most stable equilibrium state with a graphite-like structure in which flat hexagonal sheets with sp^2 bonds are layered on top of each other by an ABAB stacking sequence. In the past decade, various types of compounds containing π electrons, i.e., fullerenes,[1] nanotubes[2] and one sheet of graphite, have attracted extensive basic research because of their fascinating physical and mechanical properties by virtue of their peculiar atomic structures. Also, h-BN is one of the interesting compounds with π electrons.[3] In its mechanical properties, h-BN is similar to graphite, and it is also a typical layered material with strongly anisotropic chemical bonds, so h-BN is employed as a wear-resistant lubricant.[4] Interestingly, the electronic and optical properties of h-BN are clearly different from those of graphite. Hexagonal boron nitride is a wide-gap semiconductor with high electrical resistivities, low dielectric losses and good transmittance over a wide spectral range from visible to infrared and up to the microwave part. It also shows excellent thermal conductivity and stability, low density and high chemical inertness. By virtue of the above outstanding properties, h-BN is widely used in vacuum technology, microelectronic devices[5] and optical devices,[6] especially some special applications at high temperature.

A lot of experiments and calculations have focused on the band gap energy and band structure of h-BN. However, whether h-BN is a direct band gap semiconductor or not is not yet absolutely confirmed. Previous results indicated that the band gap energy of h-BN ranges from 3.2 to 5.97 eV.[6–9] In 2004, Watanabe *et al*[6] found that h-BN is a very promising material for ultraviolet laser devices. Based on the strong luminescence peak at 5.765 eV, they assumed that h-BN is a direct-band-gap semiconductor with a band gap of 5.971 eV. On the other hand, Arnaud *et al*[7] reported that h-BN is an indirect-band-gap semicon-

*Project supported by the National Natural Science Foundation of China (Grants Nos 60876006 and 60376007) and the Natural Science Foundation of Beijing (Grants No 4072007).
†Corresponding author. E-mail: jdeng@bjut.edu.cn

ductor. Latterly, the latest results reported by Evans *et al*[8] indicated that the quasi-direct band-gap energy in h-BN was (596 ± 0.04) eV, which was similar to the result by Watanabe. The optical band gap E_g was confirmed to be (596 ± 004) eV. Samples employed in the above research were commercially available high purity h-BN powder or single crystals grown under high pressure and high temperature (HP/HT). In fact, h-BN thin film has more significance in h-BN optical and electronic industry applications. However, the values of E_g for h-BN thin films are mainly limited the range of 3.8 to 5.2 eV.[10−12] Chen *et al* reported that the E_g of pure h-BN films deposited by a traditional radio frequency (RF) sputtering system was only 4.2 eV.[11] Noreika and Francombe[12] obtained h-BN films with E_g of 4.9–5.2 eV by a reactive sputtering system. It is still difficult to deposit h-BN thin films with an E_g close to that of bulk h-BN. To the best of our knowledge, h-BN thin films prepared by physical vapour deposition (PVD) with a band gap above 5.5 eV have not been reported. In this paper, h-BN thin film with E_g of 5.97 eV, which is close to the h-BN single crystal, was successfully prepared by RF bias magnetron sputtering and post-deposition annealing. Furthermore, variations of optical constant (absorption coefficient (α), optical band gap (E_g), refractive index (n)) and optical conductivity (σ)) of the h-BN film were investigated. Our experimental results of the optical conductivity of the h-BN films confirm previous theoretical calculations by other researchers.

2. Experimental

The h-BN films were deposited on fused silica flats and IR transparent silicon (100) wafers in the same process by the RF (13.56 MHz) bias magnetron sputtering technique. The target consisted of a single-phase 80 mm diameter hot-pressed h-BN disk with purity over 99.9%. The distance between the target and the substrate was set as 5 cm. Before sputter deposition, the substrates were cleaned in an ultrasonic bath of special cleaning solution. The vacuum chamber was initially pumped down to lower than 8×10^{-4} Pa using a turbomolecular pump and then a mixture of purified Ar (75%) and N_2 (25%) gas (corresponding in a ratio of 3:1) was introduced into the chamber. During the deposition, the pressure of the chamber was maintained at 1 Pa. A pre-sputtering process for 10 minutes was introduced prior to the formal deposition in order to further activate and clean the substrate and improve the adhesion. A low negative bias (–30 V) was applied to a molybdenum electrode under the substrates by a direct current power supply. The RF power was kept constant at 250 W throughout the whole deposition. The deposition process lasted for 1 h without extra substrate temperature control. The film thickness measured by a TENCOR alpha-step profilometer was usually kept about 320–360 nm.

The as-deposited h-BN film was labelled as film A. Film A was cut and annealed at 970 K for 1 h with a heating rate of 15 K/min, then cooled down to room temperature gradually to obtain film B. The annealing was carried out immediately after film deposition. Film B was under the protection of pure N_2 (standard atmosphere) in the whole annealing process after the chamber was evacuated to a pressure of less than 2 Pa.

The vibrational properties of the h-BN films were primarily studied by Fourier transform infrared (FTIR) spectroscopy with a WQF–310 spectrometer. The FTIR transmission measurements were carried out at normal incidence and room temperature. The transmittance Te(λ) and reflectance Re(λ) were measured as a function of incident photon wavelength λ at wavelengths between 200 and 800 nm from films deposited on fused silica using a Shimadzu UV-3101(PC) spectrophotometer at normal incidence. The light sources of the spectrophotometer were tungsten and deuterium lamps, the detectors were PM and PbS, respectively. The spectrophotometer was used in double-beam mode. The upper energy limit of the spectrophotometer is about 6.21 eV (198 nm).

3. Results and discussion

In Fig.1 curve A shows the FTIR transmittance spectrum of the film A (as-deposited) deposited on silicon substrate. A strong IR peak centred at 1372 cm^{-1} (B–N stretching) and a weak peak at 775 cm^{-1} (B–N–B bending) clearly reveal the two vibration modes of the sp^2 bond in h-BN. This indicates that film A is composed of the pure h-BN phase. The FTIR spectrum of film B (annealed at 970 K) is shown by curve B in Fig.1 A slight concavity at 1103 cm^{-1} may originate from vibration modes of other phases for curve B in Fig.1. This indicates that the h-BN film deposited by RF bias magnetron sputtering without extra substrate temperature control can maintain the available structure stability at a high temperature under atmospheric pressure.

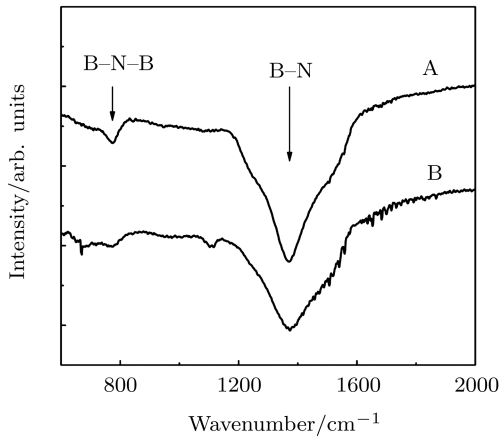


Fig.1. FTIR spectra of the RF magnetron sputtered h-BN films deposited on silicon substrate: film A as-deposited and film B annealed at 970 K for 1 h.

Figure 2 displays the optical reflectance spectra Re(λ) and transmittance spectra Te(λ) of the h-BN film A (as-deposited) and B (annealed) deposited on fused silica substrate from 200 to 800 nm. Interference phenomena are evident, as shown in the reflectance spectra Re (λ). The reflectance of film A nearly keeps a constant value around 11% from 200 to 800 nm. After annealing at 970 K, the reflectance of film B still keeps constant in the visible region, and goes up to 18% with decreasing photon wavelength λ in the ultraviolet region. From Fig.2 it is very clear that the reflectance of curve B is higher than that of curve A when $\lambda < 270$ nm, because the density of the BN film is becoming larger after being annealed so that its refractive index n is also getting larger.

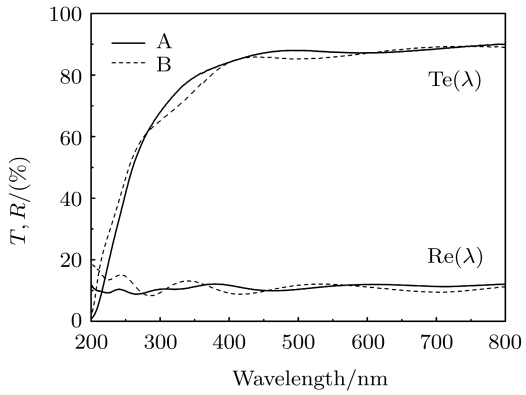


Fig.2. The transmittance spectra Te(λ) and reflectance spectra Re(λ) of the RF magnetron sputtered h-BN films deposited on fused silica substrates (A) as-deposited and (B) annealed at 970 K for 1 h.

Based on the interference theory of films, the reflectance increases with the increase of refractive index n. In transmittance spectra Te(λ), the transmittance of film B still keeps above 85% as high as that of film A within the visible region (400–760 nm), while the optical absorption edge of film B noticeably moves to high energy in the ultraviolet region. This indicates that the optical band gap E_g of h-BN film increases after 970 K annealing. Factors such as enhanced surface scattering owing to the increase of surface roughness, accumulation of boron in BN films caused by nitrogen loss and stress relaxation in film at high temperature may be used to explain why high temperature can influence the reflectance and transmittances of h-BN film in the ultraviolet region. Thermal history is clearly vital to the variation of the optical properties of h-BN films, because high temperature thermal treatment may change the structural and/or mechanical properties of the BN films. A change of structural and/or mechanical properties can lead to change in the optical properties of the BN films during annealing treatment. Figure 1 shows that no clear structural changes occur in the h-BN film B after high temperature annealing, which indicates that phase transformation is not the key factor influencing optical properties of h-BN films. On the other hand, large amounts of structural defects exist in the bias RF-sputtered h-BN films because of energetic particle bombardment by negative bias during deposition. The existence of structural defects can lead to residual stress in film A. After 970 K annealing, the structural defects can be eliminated and the residual stress can be relaxed in film B. Moreover, lots of strong evidence revealed that a close relation exists between the optical absorption edge and the stress of amorphous thin films. Kumar *et al* reported that E_g increases, i.e. blue shift of the optical absorption edge, with the decrease of stress.[13] The relation is not limited to a particular type of material but rather universal in nature. Actually in our experimental results, the clear blue shift of the optical absorption edge probably results from the stress relaxation induced by high temperature annealing. This result indicates that the variation of the stress noticeably influence the optical absorption properties of h-BN film.

The absorption coefficient α of the h-BN films can be determined by the measured optical transmittance Te(λ) and reflectance spectra Re(λ) and the following equation group[14]

$$R_e = R + \frac{R\,(1-R)^2 \exp(-2\alpha d)}{1 - R^2 \exp(-2\alpha d)}, \qquad (1)$$

$$T_e = \frac{(1-R)^2 \exp(-\alpha d)}{1 - R^2 \exp(-2\alpha d)}, \qquad (2)$$

where d is the film thickness, and in the case of normal incidence, R can be expressed simply as a function of

the refractive index n, i.e., $R = (n-1/n+1)^2$. By resolving equation group (1) and (2), we get the following computational formulas of absorption coefficient α of the h-BN films:

$$\alpha = \ln\left[\frac{1-2R_{\rm e}+R_{\rm e}^2-T_{\rm e}^2-\sqrt{4T_{\rm e}^2+\left(T_{\rm e}^2-R_{\rm e}^2+2R_{\rm e}-1\right)^2}}{2T_{\rm e}}\right]\Big/ d. \tag{3}$$

Figure 3 shows the variations of absorption coefficient α as a function of incident photon energy $h\nu$ for the h-BN films A and B. The curves are clearly divided into three regions, i.e., a low absorption region at low energy, followed by a region in which α varies exponentially as $h\nu$, and then α increases with $(h\nu)^p$ ($p = 1/2$ for a direct band gap material and $p = 2$ for an indirect band gap material) in the high energy region. This is consistent with the results of Tauc[15] who reported the intrinsic absorption spectra of amorphous semiconductors. In the weak absorption region, the intensity and shape of film absorption depending on the components, preparation of films and thermal history reflect the magnitude and distribution gap density of states.[16]

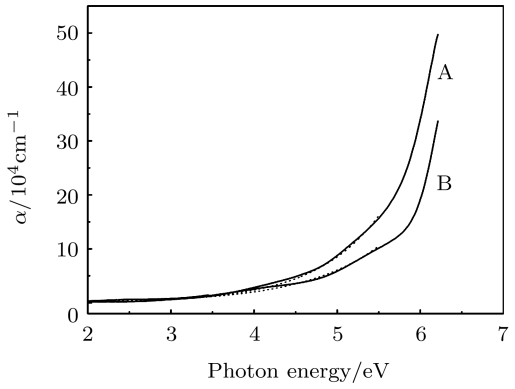


Fig.3. The absorption coefficient α calculated from the measured Te(λ), Re(λ) and Equation (3) as a function of incident photon energy $h\nu$ for the h-BN films A and B. The dashed lines are fits of the absorption tails of the films to the Urbach equation.

In amorphous semiconductors, exponentially increased absorption in the middle level energy region was first observed by Urbach.[17] It may be attributed to a broadening of states caused by the disordered structure of the films and the presence of exponentially distributed states below the absorption edge extending into the gap of the films. The exponential tail can be characterized by the Urbach expression

$$\alpha = \alpha_0 \exp\left(h\nu/E_0\right), \tag{4}$$

where α_0 is a constant, E_0 is the Urbach energy. The larger E_0 value of amorphous semiconductors relates to greater compositional or structural disorder and greater average coordination.[18] The dashed lines shown in Fig.3 show the fits of the absorption tails of the two films according to the Urbach equation. The Urbach energies of films A and B obtained from these fits are 0.78 and 0.91 eV, respectively. The increase of E_0 indicates the increase of structural disorder and average coordination in film B, which can be qualitatively inferred from the widening of the FTIR absorption peak in Fig.1.

Hexagonal BN is a direct band gap material based on the latest results reported by Evans *et al.*[8] The absorption coefficient α varies as $(h\nu)^p$ in the high energy region due to band-to-band transitions, where $p = 1/2$ for direct band gap h-BN. For films A and B, the absorption coefficient α has the form of $\alpha h\nu = K_1(h\nu - E_{\rm g})^{1/2}$, where K_1 is a material constant. The graphs of $(\alpha h\nu)^2$ versus $h\nu$ are shown in Fig.4 for the films A and B. The optical band gap $E_{\rm g}$ of 5.86 eV of film A can be given, when the linear portion of the plot $(\alpha h\nu)^2$ versus $h\nu$ is extrapolated to the $(\alpha h\nu)^2 = 0$ point. The optical band gap $E_{\rm g}$ of film B increases up to 5.97 eV after 970 K annealing. This value is considerably closer to that of h-BN single crystal.[6–8] To our knowledge, sputtered h-BN film with such a wide band gap has not been reported previously. The values of optical band gap obtained here are also very close to those of BN thin films calculated from the optical reflectance spectra Re(λ).[19]

The computational formula of the refractive index n of the BN films can be calculated from the measured optical reflectance spectra Re(λ) and transmittance spectra Te(λ) data by resolving equation group (1) and (2)

$$R = \frac{R_e^2 - 2R_e - 1 - T_e^2 + \sqrt{4R_e^2 - 8R_e + (1 + 2R_e - R_e^2 + T_e^2)^2}}{2R_e - 4}, \quad (5)$$

$$n = \frac{1 + \sqrt{R}}{1 - \sqrt{R}}. \quad (6)$$

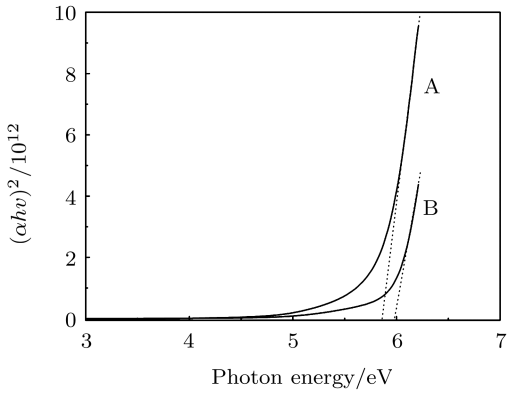


Fig.4. Determination of the optical band gap of the direct-band-gap h-BN films A and B from the plot of $(\alpha h\nu)^2$ versus $h\nu$.

Figure 5 shows variations of the refractive index n as a function of incident photon wavelength λ for films A and B. In the visible region, the refractive index of films A and B varies from 1.54 to 1.65 and 1.61 to 1.69, respectively. Similar results have also been reported by Ishii and Sato who found that the optical properties of h-BN are highly anisotropic, and the

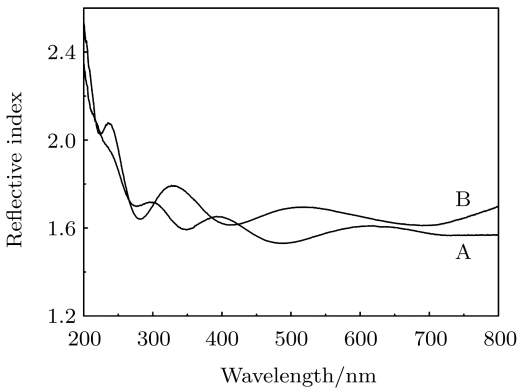


Fig.5. Variations of the refractive index n calculated from the transmittance and reflectance measurements Te(λ) and Re(λ) using Eqs.(5) and (6) as a function of incident photon wavelength λ for the h-BN films A and B.

refractive indexes parallel and perpendicular to the c axis are 2.05 and 1.65, respectively.[20] It is noticeable that the n value of the h-BN film increases after high temperature treatment, which can be attributed to the increased density of h-BN film after annealing. In the region of the absorption edge, the refractive indexes of the h-BN films increase with incident photon wavelength λ reducing to 200 nm.

Since the absorption coefficient α and refractive index n are known, the optical conductivity σ can be deduced from the following equation

$$\sigma = \frac{\alpha n c}{4\pi}. \quad (7)$$

As shown in Fig.6, the optical conductivity σ of h-BN films in the visible region is much lower than that in the high energy ultraviolet region. After annealing, the σ of h-BN film B increases and varies monotonously with incident photon wavelength λ from 760 to 400 nm. In the threshold region (energy > 4 eV), the σ of film A exceeds the σ of film B and rapidly increases to 2.78×10^{15} s^{-1}. This experimental result is completely consistent with the value calculated by Xu and Ching.[21]

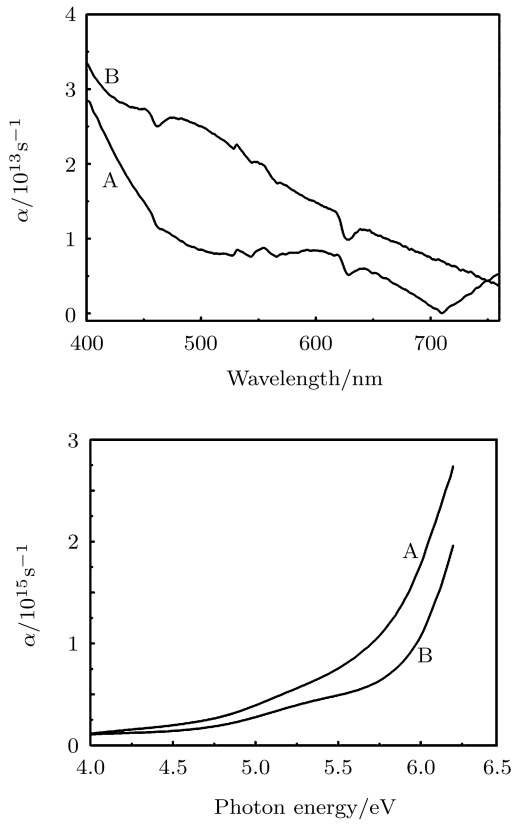


Fig.6. Optical conductivity σ of the h-BN films A and B in the visible and ultraviolet regions deduced from the absorption coefficient α, refractive index n using Eq.(7).

4. Conclusion

In this paper, the optical property variations of h-BN thin films with a high E_g comparable to that of h-BN single crystal have been studied by UV–visible transmittance and reflection measurements. The absorption edge of h-BN films shifts to high energy after 970 K annealing, which indicates an increase in E_g of the films. The change in the optical absorption probably results from stress relaxation under high temperatures. The optical absorption behaviour of h-BN films shows some characteristics of amorphous materials. The dependence of the optical absorption coefficient α on the photon energy $h\nu$ was fitted by the Urbach tail model. The E_g (5.86 eV) of as-deposited h-BN film was obtained from the fits. After annealing at 970 K for 1 h under the protection of pure N_2 at standard atmosphere, the E_g of sputtered h-BN films with available structural stability increases to 5.97 eV. In addition, the refractive index n and optical conductivity σ exhibit clearly different trends in the visible and ultraviolet regions. The experimental results confirm the previous calculations by other researchers.

References

[1] Kroto H W, Heath J R, O'Brien S C, Curl R F and Smalley R E 1985 *Nature* **318** 162

[2] Iijima S 1991 *Nature* **354** 56

[3] Oshima C and Nagashima A 1997 *J. Phys.*: *Condens. Matter* **9** 1

[4] Miyoshi K, Buckley D H, Pouch J J, Alterovitz S A and Sliney H E 1987 *Surf. Coat. Technol.* **33** 221

[5] Pauli T K, Bhattacharya P and Bose D N 1990 *Appl. Phys. Lett.* **56** 2648

[6] Watanabe K, Taniguchi T and Kanda H 2004 *Nature Materials* **3** 404

[7] Arnaud B, Lebègue S, Rabiller P and Alouani M 2006 *Phys. Rev. Lett.* **96** 026402

[8] Evans D A, McGlynn A G, Towlson B M, Gunn M, Jones D, Jenkins T E, Winter R and Poolton N R J 2008 *J. Phys.*: *Condens. Matter* **20** 075233-1

[9] Remes Z, Nesladek M, Haenen K, Watanabe K and Taniguchi T 2005 *Phys. Stat. Sol.* (a) **202** 2229

[10] Rand M J and Roberts J F 1968 *J. Electrochem. Soc.* **115** 423

[11] Chen G H, Zhang X W, Wang B, Song X M, Cui B T and Yan H 1999 *Appl. Phys. Lett.* **75** 10

[12] Noreika A J and Francombe M H 1969 *J. Vac. Sci. Technol.* **6** 722

[13] Kuma Sushil, Dixit P N, Panwar O S and Bhattacharyya R 2003 *Diamond Relat. Mater.* **12** 1576

[14] Okamoto K, Yamamoto Y, Tanaka H and Tanoka M 1984 *Bull. Chem. Soc. Jap.* **48** 2015

[15] Tauc J 1974 *Amorphous and Liquid Semiconductors* (London and New York: Plenum Press) p172

[16] Jackson W B and Amer N M 1982 *Phys. Rev.* B **25** 5559

[17] Urbach F 1953 *Phys. Rev.* **92** 1324

[18] Mott N F and Davis E A 1979 *Electronic Processes in Non-Crystalline Materials* (Oxford: Oxford Univ. Press) p283

[19] Deng J X, Wang X Y, Yao Q, Zhou T and Zhang X K 2008 *Acta Phys. Sin.* **57** 6631 (in Chinese)

[20] Ishii T and Sato T 1983 *J. Cryst. Growth* **61** 689

[21] Xu Y N and Ching W Y 1991 *Phys. Rev.* B **44** 7787